Articles

Contribution from the Baker Laboratory of Chemistry,
Cornell University, Ithaca, New York 14853

Structural and Electronic Instabilities in $M^{II}Mo_6S_8$ Compounds

D. C. JOHNSON,* J. M. TARASCON,† and M. J. SIENKO

Received August 8, 1984

The physical properties of an isoelectronic series of ternary molybdenum sulfides, $M^{II}Mo_6S_8$ (M = Ca, Sr, Ba, Yb, Eu, Sn, Pb), are reviewed. Anomalies in their physical properties indicate that electronic instabilities occur and structural instabilities may also occur in all of these phases. The transformation temperatures correlate with the second ionization potentials of the cation involved, indicating that ternary metal–sulfur bonding influences the stability of the high-temperature rhombohedral phase. Additionally, the transformation temperatures for the compounds that superconduct correlate with the observed superconducting critical temperatures and with anomalies in the pressure dependence of the superconducting critical temperature. These correlations suggest a reduction of the conduction electron density and electron–phonon coupling during the electronic and/or structural transition. These ideas are then extended to the $PbMo_6(S_{1-x}Se_x)_8$ solid solution, where anomalies in the magnetic susceptibility are reflected in the observed superconducting critical temperatures.

Introduction

One of the challenges in solid-state chemistry is to understand the physical and electronic properties of advanced materials via knowledge of the chemical bonding. Among the substances extensively subjected to this type of study have been solid-state cluster compounds exemplified by the Chevrel phases, ternary molybdenum chalcogenides of formula MMo_6X_8 (M = Pb, Ln, Cu, ...; X = S, Se, Te). These materials have been of special interest because, depending upon M, they may be high-temperature superconductors with extraordinarily high critical magnetic fields.[1] In the attempt to understand the interplay between chemical composition and properties, especially superconducting critical temperatures, a large collection of data has been accumulated on Chevrel-phase compounds and their associated solid solutions. A review of these data reveals that the highest superconducting critical temperature and among the highest critical magnetic fields occur when the ternary atom, M, is divalent and the chalcogen is sulfur (for $PbMo_6S_8$, T_c = 14 K and H_{c2} = 600 kG: for $SnMo_6S_8$, T_c = 13 K and H_{c2} = 500 kG).[2] In this investigation, we examine the physical properties of the $M^{II}Mo_6S_8$ compounds, demonstrating a link connecting the data.

The main building block of the Chevrel phases is the Mo_6X_8 unit in which a distorted cube is formed by eight chalcogen atoms at the cube corners and six molybdenum atoms sit slightly above the face centers, forming an octahedron within the chalcogen cube. Individual Mo_6X_8 units are rotated approximately 25° about the 3-fold axis of the cube so as to optimize the bonding distance between a general-position chalcogen atom of one cube and a molybdenum of an adjacent cube. The compounds discussed in this paper have the M atoms positioned between Mo_6X_8 units on the 3-fold axis. The MMo_6X_8 structure is shown in Figure 1.

The physical and electronic properties of the Chevrel phases are dominated by the intra- and intercluster molybdenum–molybdenum distances since the conduction band, as revealed by photoelectron spectra, is made up of molybdenum d orbitals.[3] The molybdenum–molybdenum intracluster distances are determined by the number of electrons available for bonding in the molybdenum octahedron. The ternary metal is generally assumed to exist in the structure as a cation, donating its electrons to the molybdenum cluster. Yvon has demonstrated that the molybdenum–molybdenum intracluster distances change with ternary metal valence, becoming shorter as the ternary metal donates more electrons to the cluster.[4] The molybdenum d band can accept up to four electrons from the ternary metal, which results in a formal valence of 2+ for the molybdenum atoms $[(M^{4+})(Mo^{2+})_6(S^{2-})_8]$ and makes 24 electrons available to form 12 molybdenum–molybdenum single bonds in the cluster. The intercluster distances are affected by the size of the ternary cation: a large cation such as Ba^{2+} expands the structure, leading to a large molybdenum–molybdenum intercluster distance.

Table I. Starting Materials for MMo_6S_8 Synthesis

element	purity, %	source
sulfur	99.9999	Atomergic Chemetals Corp.
molybdenum	99.95	United Mineral and Chemical Co.
lead	99.9999	Atomergic Chemetals Corp.
tin	99.99995	Alfa Division, Ventron Corp.
ytterbium	99.99	United Mineral and Chemical Co.

Structural phase transitions have been observed in several $M^{II}Mo_6S_8$ compounds (M = Eu, Ba, Sr, Ca).[5-7] The observed distortion results in a lowering of crystal symmetry due to a triclinic deformation of the molybdenum octahedron. These results have been interpreted as an electronic instability associated with the molybdenum-d states. Anderson, Klose, and Nohl have performed band structure calculations on rhombohedral MMo_6S_8 compounds and conclude that the conduction band has e_g symmetry and consists mainly of the molybdenum-d states of the isolated octahedron.[8] The results of Yvon suggest that these states are bonding and determine the size and shape of the octahedron.[4] For $M^{II}Mo_6S_8$ compounds, assuming perfect stoichiometry and only one conduction band, the doubly degenerate e_g band is half-filled. Baillif et al.[6] suggest that a Jahn–Teller-like electronic instability, which lifts the degeneracy and lowers the energy, is the driving force for the distortion. They point to the shortened molybdenum–molybdenum intracluster bonds as evidence of a localization of the conduction electrons in one of the split subbands.

* To whom correspondence should be addressed at E. I. du Pont de Nemours & Co., Central Research & Development Department, Experimental Station 356, Wilmington, DE 19898.
† Current address: Bell Communications Research, Murray Hill, NJ 07974.

(1) For reviews of the Chevrel phases see: Yvon, K. *Curr. Top. Mater. Sci.* **1979**, *3*, 53. Fischer, Ø. *Appl. Phys.* **1978**, *16*, 1.
(2) Foner, S.; McNiff, E. J., Jr.; Alexander, E. J. *Phys. Lett. A* **1974**, *49A*, 269.
(3) Kurmaev, C. Z.; Yarmoshenko, Y. M.; Nyholm, R.; Martensson, N.; Jarlburg, T. *Solid State Commun.* **1981**, *37*, 641.
(4) Yvon, K.; Paoli, A.; Flukiger, R.; Chevrel, R. *Acta Crystallogr., Sect. B: Struct. Crystallogr. Cryst. Chem.* **1977**, *B33*, 3066.
(5) Baillif, R.; Junod, A.; Lachal, B.; Muller, J.; Yvon, K. *Solid State Commun.* **1981**, *40*, 603.
(6) Baillif, R.; Dunand, A.; Muller, J.; Yvon, K. *Phys. Rev. Lett.* **1981**, *47*, 672.
(7) Lachal, B.; Baillif, R.; Junod, A.; Muller, J. *Solid State Commun.* **1983**, *45*, 849.
(8) Nohl, H.; Klose, W.; Anderson, O. K. "Superconductivity in Ternary Compounds"; Fischer, Ø., Maple, M. B., Eds.; Springer-Verlag: Berlin, 1982; Chapter 6.

0020-1669/85/1324-2598$01.50/0

Table II. Crystal Data for MMo_6S_8 Compounds

compd	ternary cation radius, Å	a_r, Å	α_r, deg	a_h, Å	c_h, Å	c_h/a_h	V_r, Å^3	ref
$PbMo_6S_8$	1.43	6.548 (2)	89.12 (1)	9.197 (3)	11.497 (3)	1.2500	280.7 (1)	
$SnMo_6S_8$	1.30	6.522 (2)	89.49 (1)	9.128 (3)	11.397 (3)	1.2411	277.4 (1)	
$YbMo_6S_8$	1.28	6.510 (2)	89.44 (1)	9.161 (3)	11.385 (3)	1.2427	275.8 (1)	
$EuMo_6S_8$	1.39	6.558	88.91	9.186	11.573	1.2599	281.9	5
$BaMo_6S_8$	1.56	6.648	89.0	9.31	11.70	1.257	292.7	5
$SrMo_6S_8$	1.40	6.56	89.44	9.23	11.47	1.243	282.1	2
$CaMo_6S_8$	1.26	6.50	89.77	9.17	11.30	1.232	274.3	2

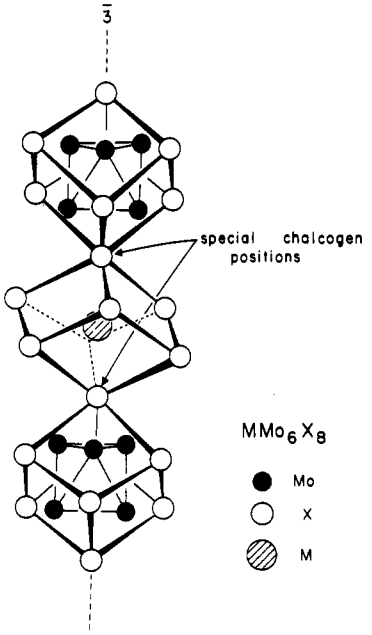

Figure 1. The Chevrel-phase structure MMo_6X_8.

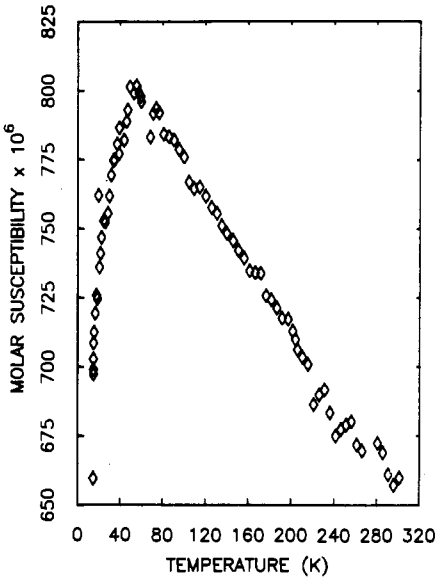

Figure 2. Magnetic susceptibility of $PbMo_6S_8$.

Recent band structure calculations on the triclinic low-temperature structure supports these conjectures.[8] In this paper we extend these ideas, showing that electronic instabilities are a common theme in $M^{II}Mo_6S_8$ compounds and showing how these instabilities correlate with the nature of the ternary metal cations and with the observed superconducting critical temperatures.

Experimental Section

Sample Preparation. Samples of $M^{II}Mo_6S_8$ (M = Sn, Pb, Yb, Eu) along with the solid solution $PbMo_6(S_{1-x}Se_x)_8$ were prepared from ultrapure starting elements, purity and sources of which are shown in Table I. Prior to use, the molybdenum powder was reduced at 1000 °C under a flow of hydrogen and stored in a vacuum desiccator.

Appropriate amounts of the elements to form 1-g samples were placed in degassed silica tubes, which were then evacuated to 10^{-6} torr and sealed. All of the tubes were placed together in a box furnace, the temperature of which was uniformly and slowly raised to 1050 °C over the course of 5 days. After 24 h at 1050 °C, the samples were cooled in air and vigorously shaken to homogenize the powder. The samples were immediately reheated to 1100 °C for 48 h and then air cooled. The samples were opened in a helium Dri-Lab and thoroughly ground. After being resealed in new degassed silica tubes, which were in turn sealed in larger ones, the samples were heated as previously described. The samples were then heated at 1200 °C for 96 h and finally air cooled. The resulting materials were fine, homogeneous gray-black powders.

Powder X-ray Diffraction. X-ray photographs were made by using a 114.6-mm-diameter Debye-Scherrer camera with nickel-filtered Cu Kα radiation. Lines were indexed with the aid of a Fortran program that calculated the positions and intensities of possible reflections from available single-crystal data. A least-squares fit, with corrections for absorption and camera radius error, was performed by using all lines with $\theta(hkl) > 30°$ that could be indexed unambiguously. The procedure yields lattice parameters with errors of less than 1 ppt.

Superconducting Transition Determination. The transition to the superconducting state was monitored by using an ac mutual-inductance apparatus, which has been described elsewhere.[9] In this device, the detection system is a primary coil with two opposed secondary coils wound symmetrically about it. The sample was placed in one of the secondary coils, and onset of superconductivity was signaled by an imbalance between the secondary coils due to an abrupt increase in magnetic shielding that occurred when the sample became perfectly diamagnetic. Temperature was measured by using a calibrated CryoCal germanium thermometer, which was checked against the boiling point of helium and the transition temperatures of lead and niobium. The T_c value was taken as the temperature at which the inductively measured transition was half-complete. The width of the transition was defined as the temperature difference between the points where the transition is 10% and 90% complete.

Magnetic Susceptibility. Magnetic susceptibilities were measured from 2 K (or T_c) to room temperature by the Faraday technique with the use of the apparatus previously described.[10] The balance was calibrated by using $HgCo(SCN)_4$ as a standard. Samples were held in Spectrosil quartz buckets. All samples were run over a range of fields (5–10 kG); susceptibilities were found to be field independent. The reported susceptibilities have been corrected for the susceptibility of the quartz buckets.

Results and Discussion

The X-ray data of the samples indicated that they were all single phased. All lines could be indexed to the appropriate rhombohedral phase. The crystal data obtained, which are listed in Table II for the MMo_6S_8 compounds, agree with previously published data.[11-13] The lattice parameters for the $PbMo_6(S_{1-x}Se_x)_8$ solid solution were consistent with those published previously.[14]

Recently, Hinks and co-workers have studied the incorporation of oxygen into the lead and tin ternary molybdenum sulfides.[15]

(9) Fisher, W. G. Ph.D. Thesis, Cornell University, 1978.

(10) Johnson, D. C. Ph.D. Thesis, Cornell University, 1983.
(11) Tarascon, J. M.; Johnson, D. C.; Sienko, M. J. *Inorg. Chem.* **1982**, *21*, 505.
(12) Johnson, D. C.; Tarascon, J. M.; Sienko, M. J. *Inorg. Chem.* **1983**, *22*, 3773.
(13) Delk, F. S., II; Sienko, M. J. *Inorg. Chem.* **1980**, *19*, 788.
(14) Delk, F. S., II; Sienko, M. J. *Inorg. Chem.* **1980**, *19*, 1352.
(15) Hinks, D. G.; Jorgensen, J. D.; Li, H. C. *Phys. Rev. Lett.* **1983**, *54*, 1981.

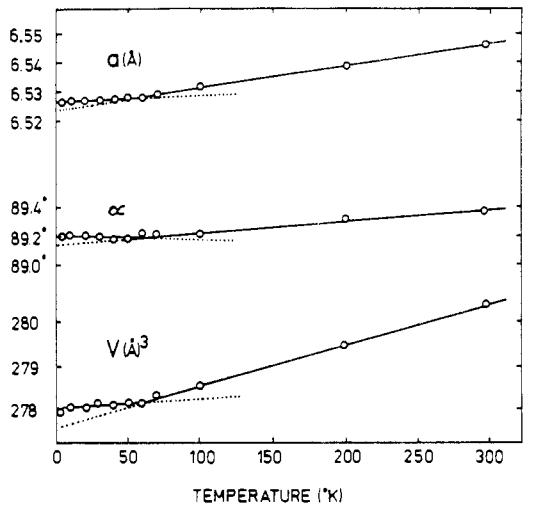

Figure 3. Rhombohedral lattice parameters as a function of temperature for $PbMo_6S_8$ (after ref 17).

From powder neutron diffraction data they find that small amounts of oxygen (up to a stoichiometry $MMo_6S_{7.8}O_{0.2}$) can replace the special-position chalcogens in the structure. This causes a displacement of the ternary metal atom toward the included oxygen and affects the lattice parameters and physical properties of the samples. The hexagonal c axis was observed to decrease with the addition of oxygen. The samples prepared in this study have hexagonal c lattice parameters that are larger by 0.03 Å than those reported by Hinks et al. for samples that nominally contain no oxygen, thus indicating that they do not have any significant oxygen impurities.

The susceptibility of $PbMo_6S_8$ is shown in Figure 2. There is a pronounced maximum in the susceptibility at approximately 60 K. This maximum corresponds with anomalies in the temperature dependence of other physical properties such as the single-crystal resistivity[16] and the lattice parameters as shown in Figure 3.[17]

These peculiarities led Shevchenko et al.[18] to investigate the low-temperature X-ray diffraction pattern of a sintered $PbMo_6S_8$ sample, and they found that all diffraction lines with $(h^2 + k^2 + l^2) \geq 9$ undergo anomalous broadening below 77 K. This broadening was reported to be reversible and was interpreted by the authors to be the onset of a lattice instability, perhaps related to a lowering of the crystal symmetry.[18] This corresponds with the observations of Baillif et al.[6] on sintered samples of $EuMo_6S_8$ and $BaMo_6S_8$, where low temperature X-ray powder patterns on sintered samples showed only line broadening while for more crystalline samples prepared from melts the low-temperature X-ray lines broadened and split as the temperature was lowered. The anomalies observed in the resistivity and specific heat of the melted europium and barium samples were also more pronounced than those found in the sintered samples.

The susceptibility and resistivity data indicate that an electronic instability occurs in $PbMo_6S_8$ at 60 K, and both the anomaly in the temperature dependence of the lattice parameters and the broadening of the powder X-ray diffraction lines indicate that a structural distortion occurs at the same temperature. In analogy with the instabilities found for $EuMo_6S_8$ and $BaMo_6S_8$, a distortion of the molybdenum octahedra is a possible cause of the observed anomalies.

The susceptibility of $YbMo_6S_8$ is shown in Figure 4. The Curie part of the susceptibility is due to a small amount of rare-earth impurity in the ytterbium metal starting material since ytterbium is divalent, $4f^{14}$ and therefore diamagnetic in $YbMo_6S_8$. If this

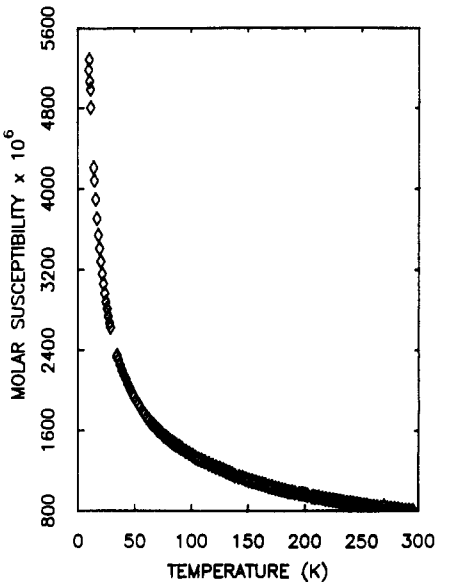

Figure 4. Magnetic susceptibility of $YbMo_6S_8$.

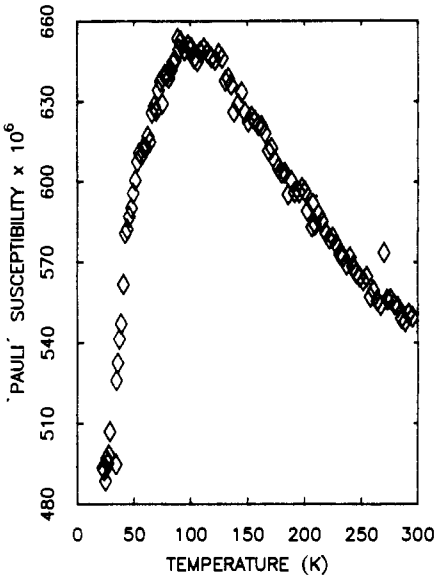

Figure 5. Magnetic susceptibility of $YbMo_6S_8$ corrected for rare-earth impurities.

Curie contribution to the susceptibility is subtracted, by fitting the low-temperature data to $\chi = C/T + \chi_0$, a temperature-dependent susceptibility similar to $PbMo_6S_8$ is obtained as shown in Figure 5. The break in this "Pauli" susceptibility occurs at approximately 110 K. $YbMo_6S_8$ has not been as extensively studied as $PbMo_6S_8$, and very little is known about the temperature dependence of its physical properties. A low-temperature powder neutron diffraction study has been performed,[19] but unfortunately only three temperatures were investigated. The powder data did not reveal any line splitting, but a sintered sample was used in the study. The line width parameter was not published with the rest of the data. The unusual temperature dependence of the magnetic susceptibility data alludes to an electronic instability at 110 K. This is supported by an anomaly in the pressure dependence of the superconducting critical temperature, which will be discussed at a later point.

$SnMo_6S_8$ also has irregularities in the temperature dependence of its physical properties that reveal an electronic change in this material and suggest that a structural distortion may occur. In addition to a change in the slope of the magnetic susceptibility

(16) Flukiger, R.; Baillif, R.; Walker, E. *Mater. Res. Bull.* **1978**, *13*, 743.
(17) Marezio, M.; Dernier, P. D.; Remeika, J. P.; Corenzwit, E.; Matthias, B. T. *Mater. Res. Bull.* **1973**, *8*, 657.
(18) Shevchenko, A. D.; Aleksandrov, O. V.; Drozdova, S. V.; Kalyuzhnaya, G. A.; Kiseleva, K. V.; Shevchuk, V. F.; Yachnemev, V. E. *Sov. J. Low Temp. Phys. (Engl. Transl.)* **1982**, *8* (7), 342.
(19) Jorgensen, J. D.; Hinks, D. G.; Noakes, D. R.; Viccaro, P. J.; Shenoy, G. K. *Phys. Rev. B* **1983**, *27*, 1465.

Table III. Physical Data for MMo_6S_8 Compounds

compd	distortion temp, K	2nd ionizn pot., eV	superconducting critical temp, K	anomaly press., kbar	ref
$PbMo_6S_8$	55	15.028	14	4	
$SnMo_6S_8$	80	14.628	13	6	
$YbMo_6S_8$	110–130	12.10	9	9	
$EuMo_6S_8$	109	11.24	10	8	5
$BaMo_6S_8$	171	10.001	7	15	36
$SrMo_6S_8$	139	11.027	6	11	38
$CaMo_6S_8$	45–100	11.868	...	...	7

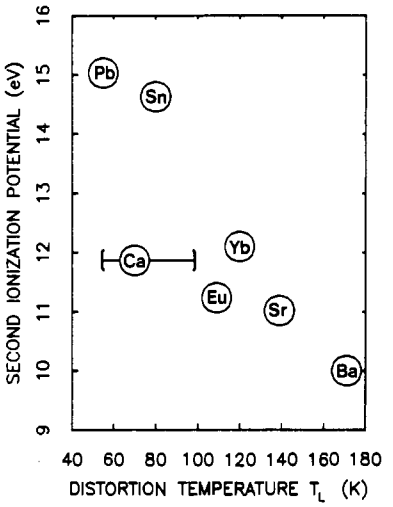

Figure 6. Second ionization potential of the ternary cation in $M^{II}Mo_6S_8$ compounds as a function of the distortion temperature, T_1.

data at 80 K, ^{119}Sn Mössbauer studies of $SnMo_6S_8$ indicate a change in the electronic environment of the tin atom. At 80 K the isomer shift abruptly decreases as the temperature is lowered, indicating that the electron density about the tin atom decreases suddenly. The data also reveal a change in the vibrational modes of the tin atom at 80 K.[20,21] The ^{119}Sn NMR data also have discontinuities in both the line width and Knight shift at 80 K, which allude to a structural change.[22]

Low-temperature X-ray measurements on $PbMo_6S_8$ are under way to confirm the break in the lattice parameters with temperature and the broadening of the diffraction lines below 77 K. These experiments will also be extended to the Sn and Yb phases to search for anomalies in their low-temperature X-ray diffraction behavior.

Table III contains a summary of the electronic instability temperatures for the Pb, Sn, and Yb phases mentioned above as well as the lattice distortion temperatures for the Eu, Ba, Sr, and Ca compounds studied previously by other researchers.[5-7] The presence of structural distortions and/or electronic anomalies in all of these $M^{II}Mo_6S_8$ compounds supports the idea of a Jahn–Teller-like electronic instability as suggested by Baillif, et al.[6] The variation of the transformation temperature with ternary metal reflects changes in the bonding of the ternary metal to the Mo_6S_8 framework. Figure 6 contains a plot of the temperature of the anomalies vs. the second ionization potential of the ternary metal cation. A rough correlation is observed: the higher the ionization potential of the ternary metal cation, the more covalent the bonding between the metal and the chalcogens. Thus the lead cation has a stronger, more covalent bond, stabilizing the high-temperature structure, than the rest of the cations. This is reflected in the thermal neutron scattering data of Schweiss et al., where

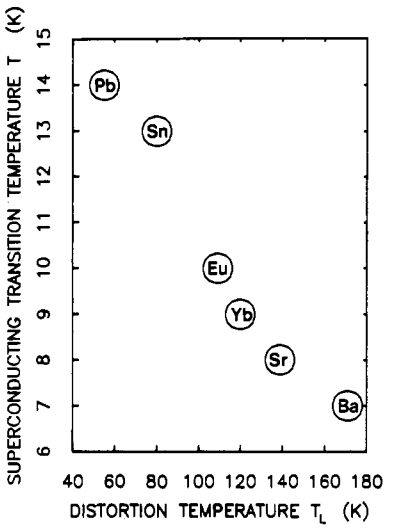

Figure 7. Superconducting critical temperature of the Sn, Yb, Sr, Ba, and Eu $M^{II}Mo_6S_8$ compounds as a function of the distortion temperature, T_1.

the lead atom in $PbMo_6S_8$ has a force constant that is 1.4 times larger than that found for tin in $SnMo_6S_8$.[23]

The europium and calcium compounds deviate the most from the trend in Figure 6. A possible cause for the deviation of $CaMo_6S_8$ is the impure nature of the sample used in the heat capacity and resistivity study that discovered the phase transition. The sample was found to contain 15–20% Mo_2S_3 as an impurity and led to the broad transition reported.[7] The stoichiometry of the sample probably differs from the ideal $CaMo_6S_8$ composition. The europium compound differs from the rest of the compounds in two respects. Europium is a magnetic cation, and the moment of the europium polarizes the conduction electrons.[12] Also, the europium compound has anomalously large lattice parameters for the size of the europium cation. The c_h axis in the europium compound is 0.10 Å larger than that observed in the lead compound, even though the lead cation is larger than the europium cation (see Table II). The general correlaton between the ionization potential and the structural distortion reflects the added stability resulting from bonding of the ternary metal cation to the chalcogen network.

The structural distortion involves localizing conduction electrons into molybdenum–molybdenum intercluster bonds and a lowering of the symmetry of the Mo_6 cluster, both tending to lower the density of states at the Fermi level. A correlation is expected between the distortion and physical properties such as the superconducting critical temperature which are related to the density of states. In the BCS theory of superconductivity,[24] the superconducting critical temperature T_c is given by

$$kT_c = \langle \hbar\omega \rangle \exp(-1/NV)$$

where $\langle\omega\rangle$ is the mean phonon frequency, N is the density of states at the Fermi level, and V is the electron–phonon coupling constant. For a high-temperature superconductor, one desires a large density of states at the Fermi level and a large electron–phonon coupling constant. Heat capacity studies have shown that the ternary molybdenum chalcogenides have high density of states,[25] and band structure calculations have shown that this is due to the symmetric Mo_6 unit and the small intercluster overlap.[8] The distortion in the $M^{II}Mo_6S_8$ compounds breaks the symmetry of the molybdenum octahedron and lowers the density of states. The electron–phonon coupling in the ternary molybdenum chalcogenides is also

(20) Kimball, C. W.; Weber, L.; VanLanduyt, G.; Fradin, F. Y.; Dunlap, B. D.; Shenoy, G. K. *Phys. Rev. Lett.* **1976**, *36*, 412.
(21) Bolz, J.; Hauck, J.; Pobell, F. *Z. Phys. B: Condens. Matter Quanta* **1976**, *25*, 351.
(22) Alekseevskii, N. E.; Nikolaev, E. G. *JETP Lett. (Engl. Transl.)* **1981**, *34*, 332.
(23) Schweiss, B. P.; Renker, B.; Schneider, E.; Reichardt, W. "Superconductivity in d- and f-Band Metals"; Douglass, D. H., Ed.; Plenum Press: New York, 1976; p 189.
(24) Bardeen, J.; Cooper, L. N.; Schrieffer, J. R. *Phys. Rev.* **1957**, *106*, 162; **1957**, *108*, 1175.
(25) Viswanathan, R.; Lawson, A. C. *Science (Washington, D.C.)* **1972**, *177*, 267.

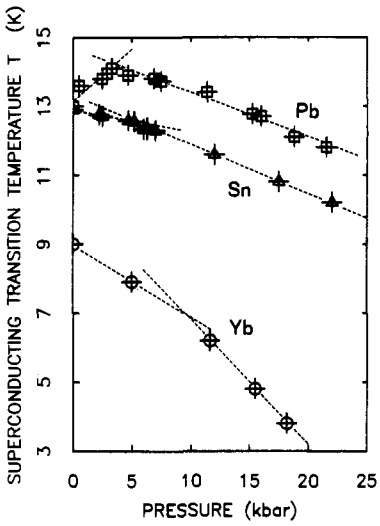

Figure 8. Pressure dependence of the superconducting critical temperature for Pb-, Sn-, and $YbMo_6S_8$ compounds (after ref 29).

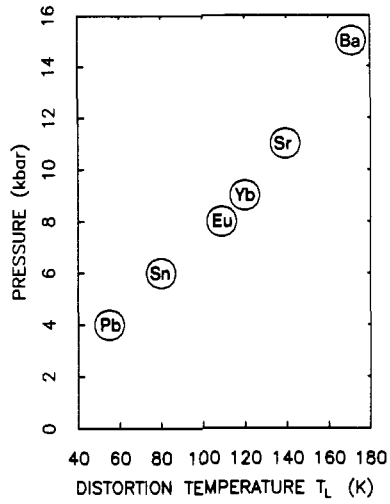

Figure 9. Pressure of the anomaly in the pressure dependence of the superconducting critical temperature as a function of the distortion temperature for $M^{II}Mo_6S_8$ compounds.

large, as evidenced by the temperature dependences of their magnetic susceptibilities[10] and the short mean free paths of the conduction electrons.[26] Large electron–phonon couplings are related to structural distortions. For the A-15 superconductors, an inverse relationship between a structural distortion, which lowers the symmetry, and the superconducting critical temperature is well documented and is postulated to be a result of an instability caused in part by the large electron–phonon coupling.[27,28]

Figure 7 contains a plot of the superconducting critical temperature vs. the temperature of the electronic and structural instabilities in the $M^{II}Mo_6S_8$ compounds. The effect of the structural and/or electronic instability upon the superconducting critical temperature is similar to that found in the A-15 compounds: the lower the transition temperature, the higher the T_c. The likely cause for this inverse relationship is that the high-temperature phase has a large coupling constant, V, causing it to be unstable at the temperature T_1. The phase below T_1 possesses a smaller electron–phonon coupling constant, which ensures its stability. If the electronic and/or structural transition could be completely suppressed, the superconducting critical temperature would be higher because of the larger V in the high-temperature phase.

The phase transition in the $M^{II}Mo_6S_8$ compounds can be suppressed by the application of pressure. The triclinic structure reported for $BaMo_6S_8$ and $EuMo_6S_8$ has a slightly larger volume than the rhombohedral structure, and when pressure is applied, the rhombohedral structure becomes energetically favored. The change in the rate of change of the volume of $PbMo_6S_8$ with temperature as shown in Figure 3 also reflects the increased stability of the high-temperature phase under pressure.

In the ternary molybdenum chalcogenides that do not have a structural distortion and/or an electronic instability, the superconducting critical temperature decreases linearly with pressure. This is due to the decrease in the volume of the material that stiffens the lattice, decreasing V. The decreased interatomic distance broadens the conduction band, which decreases the density of states. This is similar to what is observed for other materials. In fact, the superconducting transitions in lead and tin metals are used as manometers at low temperatures due to this linear behavior. The pressure dependences of the superconducting critical temperatures for Pb–, Sn–, and $YbMo_6S_8$ have been measured by Shelton[29] and are shown in Figure 8. These compounds all have an anomaly in the pressure dependence of their superconducting critical temperatures. For ytterbium and tin, this anomaly is a change in the slope dT_c/dP at a particular pressure (9 and 6 kbar), and for lead there is a rise in the superconducting critical temperature with pressure until the pressure is about 4 kbar. $EuMo_6S_8$ does not superconduct at atmospheric pressure but becomes superconducting at 7 kbar with a transition temperature of 11 K.[30–35] This anomalous behavior results from the suppression of the phase transition with pressure as observed by Chu et al.[30] by measuring the resistance of $EuMo_6S_8$ vs. temperature and pressure. Figure 9 shows a plot of the temperature of the structural distortion and/or electronic instability vs. the pressure of the anomaly in the pressure dependence of the superconducting critical temperature for the $M^{II}Mo_6S_8$ compounds.

A correlation exists between the two phenomena as shown in Figure 9, suggesting that the anomaly in the pressure dependence of the superconducting critical temperature is a result of the suppression of the structural transition and/or electronic instability. In the $M^{II}Mo_6S_8$ compounds, the electron–phonon coupling increases as the temperature is lowered until the lattice finally distorts. Once the structure distorts, the electron–phonon coupling decreases as the temperature is lowered and the distorted structure becomes stabilized. The application of pressure suppresses the distortion, stabilizing the high-temperature structure. If enough pressure is applied, the distortion is eliminated. If only a small amount of pressure is necessary to suppress the distortion, then the superconducting critical temperature actually rises as a result of the increased electron–phonon coupling as seen in the case of $PbMo_6S_8$. In this case the increase in the electron–phonon coupling and also the density of states due to suppression of the distortion is greater than the decrease of these parameters as a result of the applied pressure. In ytterbium and tin, the change in slope, dT_c/dP, indicates the point at which the distortion is completely suppressed. At higher pressures, the slope increases because there is no longer the increase in the parameters due to the distortion being suppressed.

The situation in $EuMo_6S_8$ is complicated by the magnetic moment of the europium cation. Analogous to the case of Sn-

(26) Woollam, J. A.; Alterovitz, S. A. *Solid State Commun.* **1978**, *27*, 669.
(27) Matthias, B. T. "Superconductivity in d- and f-Band Metals"; Douglass, D. H., Ed.; Plenum Press: New York, 1972; p 367.
(28) Testardi, L. R. *Comments Solid State Phys.* **1975**, *6*, 131.
(29) Shelton, R. N. Ph.D. Thesis, University of California, San Diego, 1975.
(30) Chu, C. W.; Haung, S. Z.; Lin, C. H.; Meng, R. L.; Wu, M. K. *Phys. Rev. Lett.* **1981**, *46*, 276.
(31) Harrison, D. W.; Lim, K. C.; Thompson, J. D.; Haung, C. Y.; Hambourger, P. D.; Luo, H. L. *Phys. Rev. Lett.* **1981**, *46*, 280.
(32) (a) Torikachvili, M. S.; Maple, M. B. *Physica B+C (Amsterdam)* **1981**, *108B+C*, 1271. (b) McCallum, R. W.; Kalsbach, W. A.; Radhakrishnan, T. S.; Pobell, R.; Shelton, R. N. Klavins, P. *Solid State Commun.* **1982**, *42*, 819.
(33) Wu, M. K.; Hor, P. H.; Meng, R. L.; Lin, T. H.; Diatschenko, V.; Shao, X. Y.; Jin, X. C.; Chu, C. W. *Phys. Rev. B: Condens. Matter* **1982**, *26*, 5230.
(34) Lacoe, R. C.; Wolf, S. A.; Chaikin, P. M.; Haung, C. Y.; Luo, H. L. *Phys. Rev. Lett.* **1982**, *48*, 1212.
(35) Tarascon, J. M.; Harrison, M. R.; Johnson, D. C.; Sienko, M. J. *Inorg. Chem.* **1984**, *23*, 1094.

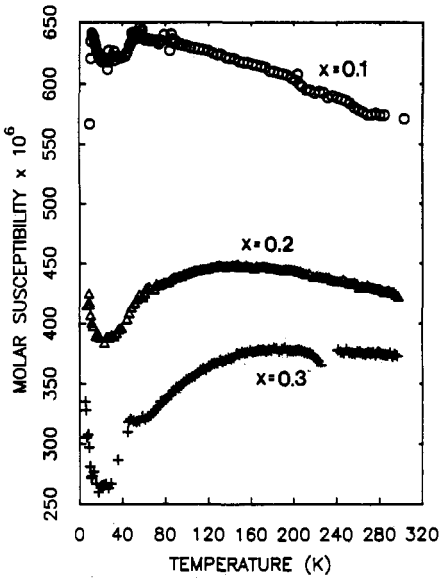

Figure 10. Magnetic susceptibility of the $PbMo_6(S_{1-x}Se_x)_8$ solid solution when x = 0.1–0.3.

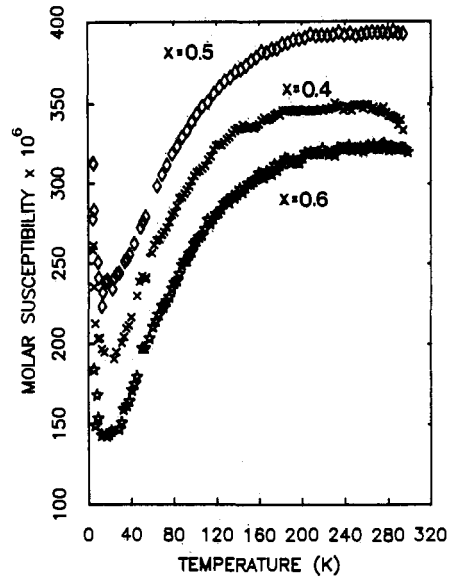

Figure 11. Magnetic susceptibility of the $PbMo_6(S_{1-x}Se_x)_8$ solid solution when x = 0.4–0.6.

Mo_6S_8, an increase in the conduction electron density at the europium cation probably occurs upon distortion. Indeed, the europium–conduction electron interaction is found by ESR to be 10 times stronger than found in other $LnMo_6S_8$ compounds.[35] This interaction may be the driving force for the metal–semiconductor transition in this material since the other MMo_6S_8 phases remain metals after the distortion.[7] Almost a complete suppression of the structural distortion is necessary before $EuMo_6S_8$ becomes superconducting, as the resistivity data as a function of pressure demonstrates.[30]

The lack of superconductivity in the Ca-, Sr-, and $BaMo_6S_8$ compounds has been explained by the presence of the structural distortion.[6] If the structural distortion is suppressed by pressure in these compounds, then they would be expected to become superconducting at higher pressures. Chu has reported the detection of a "diamagnetic" anomaly and a sudden drop in the resistivity in a sample of $BaMo_6S_8$ at a pressure of 15 kbar, which was identified as a possible superconducting transition.[36,37] Kalsbach has reported a vanishing resistivity for $SrMo_6S_8$ accompanied by an ac diamagnetic signal characteristic of the superconducting state at a pressure of 12 kbar.[38] The ionic bonding of the alkaline-earth elements in these materials may also contribute to the lack of superconductivity. The ionic bonding changes the hybridization of the orbitals involving the molybdenum and sulfur, which could lower the density of the states and also affect the electron–phonon coupling by altering the vibrational modes of the cluster units. Further experiments on these materials are necessary to determine the effects of pressure on these compounds and to confirm whether the application of pressure causes them to become superconducting.

The relationship between electronic instabilities and superconductivity can be extended to the $PbMo_6(S_{1-x}Se_x)_8$ solid solution. The magnetic susceptibility of these samples decreases below a temperature T_1 (Figures 2 and 10–12) and possibly results from an electronic instability and/or a structural distortion in analogy to $PbMo_6S_8$. The temperature of the anomaly, T_1, does not vary monotonically across the solid solution but instead follows changes in the crystallography that result from the substitution.[38] As selenium is initially substituted for sulfur, it occupies the general-position chalcogen sites, producing an unsymmetric environment about the molybdenum octahedron. This unsymmetric environment causes the electronic instability at a higher temperature. The instability occurs at a maximum temperature of 200 K for the compositions x = 0.4–0.6, which have the maximum disorder in general-position occupation. As more selenium is substituted, the transition moves to lower temperatures as all of the general-position sites become occupied by selenium, resulting

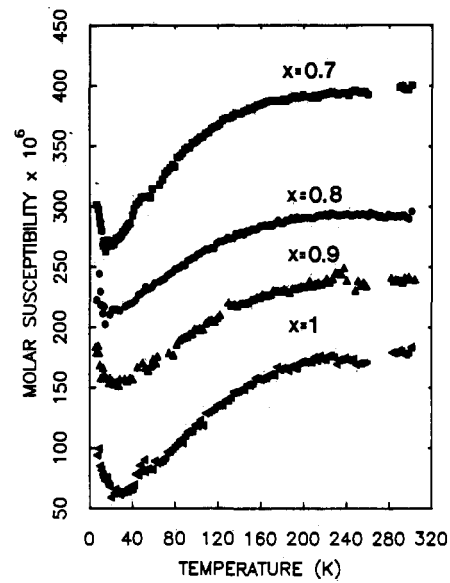

Figure 12. Magnetic susceptibility of the rest of the $PbMo_6(S_{1-x}Se_x)_8$ solid solution (x = 0.7–1.0).

Table IV. Distortion Temperature and Superconducting Critical Temperature for the $PbMo_6(S_{1-x}Se_x)_8$ Solid Solution

compound	distortion temp, K	superconducting critical temp, K
$PbMo_6S_8$	~55	14.0
$PbMo_6(S_{0.9}Se_{0.1})_8$	~70	8.95
$PbMo_6(S_{0.8}Se_{0.2})_8$	~150	6.26
$PbMo_6(S_{0.7}Se_{0.3})_8$	~170	4.58
$PbMo_6(S_{0.6}Se_{0.4})_8$	~185	3.41
$PbMo_6(S_{0.5}Se_{0.5})_8$	~200	3.52
$PbMo_6(S_{0.4}Se_{0.6})_8$	~190	3.62
$PbMo_6(S_{0.3}Se_{0.7})_8$	~160	5.08
$PbMo_6(S_{0.2}Se_{0.8})_8$	~170	6.09
$PbMo_6(S_{0.1}Se_{0.9})_8$	~180	5.55
$PbMo_6Se_8$	~190	3.89

(36) Hor, P. H.; Wu, M. K.; Lin, T. H.; Shao, X. Y.; Jin, X. C.; Chu, C. W. *Solid State Commun.* **1982**, *44*, 1605.
(37) Chu, C. W.; Wu, M. K.; Hor, P. H.; Jin, X. C. "Superconductivity in d- and f-Band Metals"; Buckel, W., Weber, W, Eds.; Kernforschungszentrum Karlsruhe GmbH: Karlsruhe, DDR, 1982; p 179.
(38) Kalsbach, W. A.; McCallum, R. W.; Poppe, U.; Pobel, F.; Shelton, R. N.; Klavins, P. "Superconductivity in d- and f-Band Metals"; Buckel, W., Weber, W., Eds.; Kernforschungszentrum Karlsruhe GmbH: Karlsruhe, DDR, 1982; p 185.

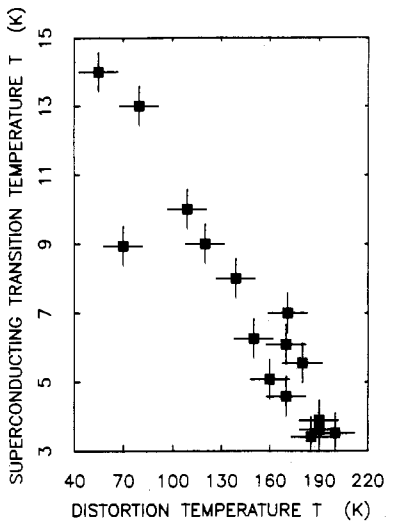

Figure 13. Superconducting critical temperature of the lead solid solution and the $M^{II}Mo_6S_8$ compounds as a function of the distortion temperature.

in a more symmetric environment about the Mo_6 cluster. These data are summarized in Table IV. Figure 13 contains a plot of the temperature of the anomaly, T_1, vs. the superconducting critical temperature for the solid solution as well as the data for Eu, Yb, Sr, Ba, and Sn. The correlation supports the hypothesis that the drops in the susceptibility are due to electronic instabilities that are related to the structural distortions observed in Eu, Sn, Ba, and Ca compounds.

By way of summary, a structural distortion in the $M^{II}Mo_6S_8$ compounds from a rhombohedral to a triclinic structure as reported by Baillif et al.[5] for the europium, barium, strontium, and calcium compounds was related to electronic instabilities in the lead, tin, and ytterbium compounds. A correlation between the temperature of the anomalies in the physical properties and the second ionization potential of the cation was demonstrated and explained in terms of increased covalent bonding of the ternary cation as the ionization potential increases. The anomaly was then shown to correlate with the superconducting critical temperatures of these compounds and also with anomalies in the pressure dependence of the superconducting critical temperature. This relationship results from the effects of electron–phonon coupling affecting both the superconducting critical temperature and the structural distortion. The correlation was extended to the $PbMo_6(S_{1-x}Se_x)_8$ solid solution, where anomalies in the magnetic susceptibility were shown to correlate with the superconducting critical temperature. This paper extends the relationship between structural and electronic instabilities and high-temperature superconductivity to yet another class of compounds.

Acknowledgment. This research was sponsored by the Air Force Office of Scientific Research, Grant No. AFOSR 80-0009, and was supported in part by the National Science Foundation and the Materials Science Center at Cornell University.

Note Added in Proof. A recent publication (Jorgensen, J. D.; Hinks, D. G. *Solid State Commun.* **1985**, *53*, 289) confirms the presence of a structural distortion in $PbMo_6S_8$ and $SnMo_6S_8$ below 100 K.

Registry No. $CaMo_6S_8$, 85714-04-1; $SrMo_6S_8$, 85704-51-4; $BaMo_6S_8$, 96866-36-3; $YbMo_6S_8$, 57485-88-8; $EuMo_6S_8$, 61642-20-4; $SnMo_6S_8$, 39432-50-3; $PbMo_6S_8$, 39432-49-0.

Contribution from the Max-Planck-Institut
für Festkörperforschung, 7000 Stuttgart-80, FRG

Interstitial Carbon Molecules, Metal–Metal Bonds, and Chemical Binding in $Gd_{10}C_4Cl_{18}$

S. SATPATHY* and O. K. ANDERSEN

Received August 22, 1984

By means of electronic structure calculations we study the chemical binding in the cluster $Gd_{10}C_4Cl_{18}$—a cluster that consists of a Gd edge-sharing double octahedron with Cl atoms bridging the remaining edges and with C_2 molecules occurring at the octahedral centers. This type of cluster is the basic unit of three compounds, $Gd_{10}C_4Cl_{18}$, $Gd_{10}C_4Cl_{17}$, and $Gd_{12}C_6I_{17}$. We find that in the $Gd_{10}C_4Cl_{18}$ cluster the Cl-like and the C_2 π_p*-like levels are occupied while the C_2 σ_p*-like and all Gd-like levels are empty. The cluster has no metal–metal bonds in the sense that there are no occupied molecular orbitals that are primarily metal–metal bonding in character. However, 1.7 electrons are contributed to each Gd atom through back-bonding from the occupied Cl-like (1.0 electron/Gd) and C_2-like (0.7 electron/Gd) states. The lowest unoccupied molecular orbital is a Gd molecular orbital in the basal plane—and concentrated along the shared edge—of the double octahedron. We expect that the binding in the cluster compound $Gd_{10}C_4Cl_{18}$ is like that in the isolated cluster and hence is predominantly ionic. For the cluster compounds $Gd_{10}C_4Cl_{17}$ and $Gd_{12}C_6I_{17}$ we find that the molecular-orbital schemes are essentially the same as in $Gd_{10}C_4Cl_{18}$; however, now an extra electron occupies the metal–metal bond concentrated along shared edges in the compound.

Introduction

Recently a novel class of cluster compounds involving rare-earth halides and carbon atoms has been synthesized.[1-4] The basic structural unit, $Gd_{10}C_4X_{18}$, of the compounds with which we shall be concerned is an edge-sharing double octahedron, $(Gd_4Gd_{2/2})_2 = Gd_{10}$, with halogen atoms, X_{18}, bridging the remaining edges of the double octahedron and with a C_2 molecule at the center of each octahedron (Figure 1). The occurrence of a molecule inside the metal octahedron is an unusual feature of these compounds. The two molecules of the double octahedron are well separated and, for each molecule, the C–C distance of 147 pm is slightly shorter than the C_2 single-bond length of 154 pm.

The crystal structures are such that the halogen atoms together with the C_2-containing Gd_6 octahedra form a face-centered cubic lattice. In the compounds $Gd_{10}C_4Cl_{18}$ and $Gd_{10}C_4Cl_{17}$ the clusters are well separated as far as distances between metal atoms are concerned: ($d^{inter}_{Gd-Gd} \geq 1.17$, $d^{intra}_{Gd-Gd} \approx 440$ pm). In $Gd_{10}C_4Cl_{17}$ two Cl atoms are shared between neighboring clusters.[2,3] In $Gd_{12}C_6I_{17}$ the double octahedra are parallel and are arranged in such a way that through the addition of linear Gd–C–C–Gd units between them third octahedra are formed, and the entire structure is then

(1) Simon, A. *Angew. Chem., Int. Ed. Engl.* **1981**, *20*, 1 and references therein.
(2) Simon, A.; Warkentin, E.; Masse, R. *Angew. Chem.* **1981**, *93*, 1071.
(3) Warkentin, E.; Masse, R.; Simon, A. *Z. Anorg. Allg. Chem.* **1982**, *491*, 323.
(4) Simon, A.; Warkentin, E. *Z. Anorg. Allg. Chem.* **1983**, *497*, 79.

0020-1669/85/1324-2604$01.50/0